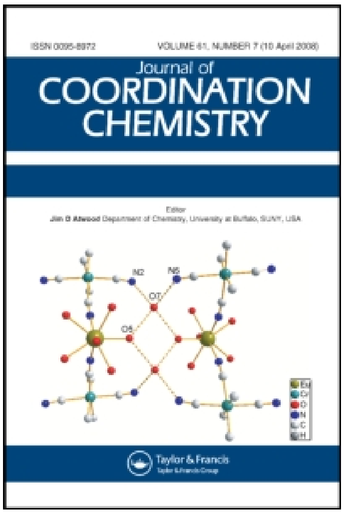

Journal of Coordination Chemistry
Publication details, including instructions for authors and subscription information:
http://www.informaworld.com/smpp/title~content=t713455674

Hydrothermal synthesis and structure of an open-framework vanadium-manganese phosphate $[C_4H_{12}N_2]_2Mn^{II}(V^VO_2)_2(V\_2^{IV}O_2)(PO_4)_4(H_2O)_4$

Yin-Zhuang Zhou[a]; Jin-Li Liu[a]; Hai-Ping Qiao[a]; Jing-Nan Feng[a]
[a] Department of Chemistry, Capital Normal University, Beijing, P.R. China

To cite this Article Zhou, Yin-Zhuang , Liu, Jin-Li , Qiao, Hai-Ping and Feng, Jing-Nan(2009) 'Hydrothermal synthesis and structure of an open-framework vanadium-manganese phosphate $[C_4H_{12}N_2]_2Mn^{II}(V^VO_2)_2(V\_2^{IV}O_2)(PO_4)_4(H_2O)_4$', Journal of Coordination Chemistry, 62: 17, 2842 — 2850

To link to this Article: DOI: 10.1080/00958970902874284

URL: http://dx.doi.org/10.1080/00958970902874284

Journal of Coordination Chemistry
Vol. 62, No. 17, 10 September 2009, 2842–2850

Taylor & Francis
Taylor & Francis Group

Hydrothermal synthesis and structure of an open-framework vanadium-manganese phosphate $[C_4H_{12}N_2]_2Mn^{II}(V^VO_2)_2(V_2^{IV}O_2)(PO_4)_4(H_2O)_4$

YIN-ZHUANG ZHOU*, JIN-LI LIU, HAI-PING QIAO and JING-NAN FENG

Department of Chemistry, Capital Normal University, Beijing, 100048, P.R. China

(*Received 4 October 2008; in final form 19 December 2008*)

A 3-D vanadium-manganese phosphate, $[C_4H_{12}N_2]_2Mn^{II}(V^VO_2)_2(V_2^{IV}O_2)(PO_4)_4(H_2O)_4$ (**1**), was synthesized hydrothermally and characterized by single crystal X-ray diffraction. This complex crystallizes in the triclinic system with the space group $P\bar{1}$ and cell parameters $a = 7.070(2)$ Å, $b = 12.356(4)$ Å, $c = 17.120(6)$ Å, $\alpha = 75.698(9)^\circ$, $\beta = 85.651(12)^\circ$, $\gamma = 78.331(10)^\circ$, and $Z = 2$. The 3-D vanadium-manganese phosphate formed from V^{IV} octahedral chains and V^V–Mn^{II}–V^V clusters, which are linked via PO_4 tetrahedra. Complex **1** contains channels in three directions in which diprotonated piperazine ions and water molecules reside. Characterization by element analysis, IR, XPS, fluorescence spectrum, and TG analysis are also described.

Keywords: Vanadium-manganese phosphate; Hydrothermal synthesis; Channel; Piperazine

1. Introduction

After the discovery of microporous aluminophosphates, considerable effort has been directed towards the synthesis of new open-framework transition-metal phosphates due to their rich structural diversity and potential applications in catalysis, adsorption, ionic conduction, ion exchange, separation, and electronics [1]. Hydrothermal synthesis has been successful for the preparation of microporous materials and other important solids. A variety of 1-D chain [2, 3], 2-D layer [2, 4, 5], and 3-D open-framework structure [1, 7–9] of vanadium phosphates were prepared in the presence of organic amines and piperazine or metal complex as structure-directing agents. Transition metals take part in vanadium phosphate oxide skeletons [5], giving two different transition metals in the phosphate compound with properties not consistent with the properties of the monometallic phosphate. The secondary metal ions exert significant influence on the topology of oxovanadium phosphates [6]. In this article, we report hydrothermal synthesis and characterization of a mixed-valence (IV/V), 3-D vanadium-manganese phosphate $[C_4H_{12}N_2]_2Mn^{II}(V^VO_2)_2(V_2^{IV}O_2)(PO_4)_4(H_2O)_4$ (**1**). Generally, mixed-valence vanadium phosphates are more interesting than single-valence vanadium phosphates because they may show redox catalysis and unusual magnetic behavior [8]. There are

---

*Corresponding author. Email: zhouyz7813@x263.net

Journal of Coordination Chemistry
ISSN 0095-8972 print/ISSN 1029-0389 online © 2009 Taylor & Francis
DOI: 10.1080/00958970902874284

two types of building blocks in **1**, infinite $(–O–V^{IV}–)_\infty$ chains constructed from VO_6 octahedra and $V^V–Mn^{II}–V^V$ clusters. These two types of building blocks are connected by PO_4 tetrahedra to form a 3-D framework with channels in three dimensions in which diprotonated piperazine ions and water molecules reside.

2. Experimental

2.1. *General considerations*

All chemicals were commercially purchased and used without purification. Elemental analyses (C, H, and N) were performed on a Perkin-Elmer 2400 CHN Elemental Analyzer. An IR spectrum was recorded from 400–4000 cm^{-1} on a Nicolet Impact 410 FTIR Spectrophotometer using KBr pellets. A Perkin-Elmer TGA 7 thermogravimetric analyzer was used to obtain thermogravimetric (TGA) curves in air with a heating rate of 10°C min^{-1}. Emission/excitation spectra were recorded on an F-4500 FL fluorescence spectrophotometer at 293.0 K. XPS analysis was performed on a VG ESCALAB MK II spectrometer with a Mg-Kα (1253.6 eV) achromatic X-ray source. The vacuum inside the analysis chamber was maintained at 6.2×10^{-6} Pa during analysis.

2.2. *Synthesis of* $[C_4H_{12}N_2]_2Mn^{II}(V^VO_2)_2(V_2^{IV}O_2)(PO_4)_4(H_2O)_4$ *(1)*

A mixture of NH_4VO_3 (0.117 g, 1 mmol), $Mn(CH_3COO)_2 \cdot 4H_2O$ (0.245 g, 1 mmol), piperazine $\cdot$ $6H_2O$ (pip, 0.583 g, 3 mmol), H_3PO_4 (85%, 0.3 mL, 5 mmol), and H_2O (7 mL, 389 mmol) in the mole ratio 1 : 1 : 3 : 5 : 389 was placed in a 20 mL Teflon-lined stainless steel autoclave and heated at 160°C for 5 days under autogenous pressure and then cooled to room temperature at 10°C h^{-1}. Brown needle crystals of **1** suitable for X-ray analysis were harvested in 60% yield (based on vanadium). Crystals were obtained from a mixture of V_2O_5 (0.091 g, 0.5 mmol), pip (0.280 g, 1.5 mmol), $Mn(CH_3COO)_2 \cdot 4H_2O$ (0.245 g, 1 mmol), H_3PO_4 (0.3 mL, 5 mmol), and H_2O (7 mL) one time, but the procedure could not be repeated. Complex **1** was prepared in high yield when changing from V_2O_5 to NH_4VO_3 and the ratio to 1 : 1 : 3 : 5 : 389. Anal. Calcd for $C_8H_{32}MnN_4O_{26}P_4V_4$ (%): C, 9.77; H, 3.28; N, 5.70. Found: C, 9.59; H, 3.01; N, 5.39.

2.3. *Single crystal X-ray analyses*

A suitable single crystal (size: $0.32 \times 0.12 \times 0.04\ mm^3$) was carefully selected under a microscope. Crystal structure determinations for **1** were performed on a Bruker SMART-CCD X-ray single diffractometer at 294(2) K using graphite monochromated Mo-Kα radiation ($\lambda = 0.71070$ Å). Cell parameters were obtained by global refinement of the positions of all collected reflections. An empirical absorption correction was applied. The structures were solved by direct methods and refined by full-matrix least-squares on F^2 using SHELXL-97 [10, 11]. All non-hydrogen atoms were refined anisotropically; all hydrogen atoms were added theoretically. Some relevant

Table 1. Crystal data and structure refinement for **1**.

Empirical formula	$C_8H_{32}MnN_4O_{26}P_4V_4$
Formula weight	982.96
Crystal size (mm^3)	$0.32 \times 0.12 \times 0.04$
Temperature (K)	294(2)
Wavelength (Å)	0.71070
Crystal system	Triclinic
Space group	$P\bar{1}$
Unit cell dimension (Å, °)	
a	7.070(2)
b	12.356(4)
c	17.120(6)
α	75.698(9)
β	85.651(12)
γ	78.331(10)
Z	2
Calculated density ($Mg\ m^{-3}$)	2.301
Absorption coefficient (mm^{-1})	2.043
$F(000)$	986
θ range (°)	1.73–27.88
Limiting indices	$-9 \le h \le 7$ $-16 \le k \le 16$ $-22 \le l \le 22$
Reflections collected	12,609
Absorption correction	Semi-empirical
Maximum and minimum transmission	0.9227 and 0.5609
Refinement method	Full-matrix least-squares on F^2
Data/restraints/parameters	6646/0/424
Goodness-of-fit on F^2	1.156
Final R indices [$I > 2\sigma(I)$]	$R_1 = 0.0547$, $wR_2 = 0.1368$
R indices (all data)	$R_1 = 0.0928$, $wR_2 = 0.1514$
Largest difference peak and hole ($e\,Å^{-3}$)	1.735 and –2.984

$R_1 = \sum ||F_o| - |F_c|| / \sum |F_o|$; $\omega R_2 = \{\sum \omega(F_o^2 - F_c^2)^2 / \sum \omega(F_o^2)^2\}^{1/2}$.

crystallographic data and structure determination parameters are summarized in table 1. Selected bond lengths and angles for **1** are given in table 2.

3. Results and discussion

3.1. *Structure description*

As shown in figure 1, **1** has a $Mn^{II}(V^{V}O_2)_2(V_2^{IV}O_2)(PO_4)_4(H_2O)_2^{4-}$ skeleton and contains diprotonated piperazine cations and water. The $Mn^{II}(V^{V}O_2)_2(V_2^{IV}O_2)(PO_4)_4(H_2O)_2^{4-}$ framework is constructed by $V^{V}O_5$ square pyramids, $V^{IV}O_6$ octahedra, PO_4 tetrahedra, and $Mn^{II}O_4(H_2O)_2$ octahedra. The Mn^{II} sites adopt a relatively regular octahedral coordination with Mn–O distances ranging from 2.120 to 2.174 Å and O–Mn–O angles being close to 90° (87.11–92.88°) and 180° (179.62–179.8°). Four crystallographically distinct vanadiums have two different coordination geometries. $V^{V}(1)O_5$ and $V^{V}(2)O_5$ square pyramids have two short V=O bonds (1.603–1.656 Å) and three intermediate V–O bonds (1.911–2.059 Å). $V^{IV}(3)O_6$ and $V^{IV}(4)O_6$ octahedra have six V–O bonds (1.807–2.016 Å). All the P–O bonds of PO_4 tetrahedra are in the range 1.513–1.562 Å and O–P–O angles are in the range 98.07–113.5°.

Table 2. Selected bond lengths (Å) and angles (°) for **1**.

Mn(1)–O(18)	2.120(4)	Mn(1)–O(17)	2.127(4)	Mn(1)–O(21)	2.142(4)
Mn(1)–O(23)	2.146(4)	Mn(1)–O(12)#1	2.169(4)	Mn(1)–O(1)	2.174(4)
V(1)–O(20)	1.611(4)	V(1)–O(21)	1.653(4)	V(1)–O(11)#1	1.911(4)
V(1)–O(8)#2	2.009(4)	V(1)–O(7)#2	2.059(4)	V(2)–O(24)	1.603(4)
V(2)–O(23)	1.656(4)	V(2)–O(3)	1.902(4)	V(2)–O(14)	2.016(4)
V(2)–O(15)	2.050(3)	V(3)–O(19)	1.811(4)	V(3)–O(9)	1.980(4)
V(3)–O(2)	1.986(4)	V(3)–O(5)	1.992(3)	V(3)–O(16)	1.998(3)
V(3)–O(22)#4	2.016(4)	V(4)–O(22)	1.807(4)	V(4)–O(13)	1.965(4)
V(4)–O(10)	1.982(4)	V(4)–O(4)#5	1.984(4)	V(4)–O(6)	1.999(4)
V(4)–O(19)	2.016(4)	P(1)–O(1)	1.526(4)	P(1)–O(2)	1.530(4)
P(1)–O(4)	1.546(4)	P(1)–O(3)	1.559(4)		
O(18)–Mn(1)–O(17)	179.78(17)	O(18)–Mn(1)–O(21)	92.53(15)	O(17)–Mn(1)–O(21)	87.69(15)
O(18)–Mn(1)–O(23)	87.39(16)	O(17)–Mn(1)–O(23)	92.40(16)	O(21)–Mn(1)–O(23)	179.8(2)
O(18)–Mn(1)–O(12)#1	87.49(16)	O(17)–Mn(1)–O(12)#1	92.52(16)	O(21)–Mn(1)–O(12)#1	88.54(14)
O(23)–Mn(1)–O(12)#1	91.59(14)	O(18)–Mn(1)–O(1)	92.88(17)	O(17)–Mn(1)–O(1)	87.11(16)
O(21)–Mn(1)–O(1)	91.37(14)	O(23)–Mn(1)–O(1)	88.51(14)	O(12)#1–Mn(1)–O(1)	179.62(17)
O(20)–V(1)–O(21)	107.5(2)	O(20)–V(1)–O(11)#1	104.3(2)	O(21)–V(1)–O(11)#1	97.03(18)
O(20)–V(1)–O(8)#2	104.22(19)	O(21)–V(1)–O(8)#2	94.07(17)	O(11)#1–V(1)–O(8)#2	144.52(16)
O(20)–V(1)–O(7)#2	107.85(17)	O(21)–V(1)–O(7)#2	143.97(18)	O(11)#1–V(1)–O(7)#2	80.94(15)
O(8)#2–V(1)–O(7)#2	70.55(15)	O(19)–V(3)–O(9)	92.61(17)	O(19)–V(3)–O(2)	94.32(17)
O(9)–V(3)–O(2)	173.07(19)	O(19)–V(3)–O(5)	92.83(16)	O(9)–V(3)–O(5)	90.78(15)
O(2)–V(3)–O(5)	88.65(16)	O(19)–V(3)–O(16)	94.41(15)	O(9)–V(3)–O(16)	88.75(16)
O(2)–V(3)–O(16)	90.95(15)	O(5)–V(3)–O(16)	172.76(19)	O(19)–V(3)–O(22)#4	179.3(2)
O(9)–V(3)–O(22)#4	86.82(15)	O(2)–V(3)–O(22)#4	86.25(16)	O(5)–V(3)–O(22)#4	86.75(15)
O(16)–V(3)–O(22)#4	86.01(14)	O(1)–P(1)–O(2)	112.2(2)	O(1)–P(1)–O(4)	108.2(2)
O(2)–P(1)–O(4)	109.8(2)	O(1)–P(1)–O(3)	110.3(2)	O(2)–P(1)–O(3)	108.7(2)
O(4)–P(1)–O(3)	107.6(2)	O(6)–P(2)–O(5)	111.8(2)	O(6)–P(2)–O(7)	110.0(2)
O(5)–P(2)–O(7)	113.5(2)	O(6)–P(2)–O(8)	109.6(2)	O(5)–P(2)–O(8)	112.9(2)
O(7)–P(2)–O(8)	98.2(2)				

Symmetry transformations used to generate equivalent atoms: #1: x, #y–1, #z; #2: $-x+1$, #$-y$,$-z+1$; #3: $-x+1$, #$-y$, #$-z+2$; #4: x–1, #y, z; #5: $x+1$, #y, #z; #6: x, #$y+1$, z; #7: $-x+1$, #$-y+2$, #$-z+2$; #8: $-x$, #$-y$, #$-z+1$; #9: $-x$, #$-y+1$, #$-z+1$; #10: $-x+1$, #$-y+1$, #$-z+2$.

As shown in figure 2, two types of building blocks are formed, vanadate chains constructed from V^{IV} octahedra (figure 2a and 2b) and V^{V}–Mn^{II}–V^{V} clusters constructed from two V^{V} square pyramids and one Mn^{II} octahedron (figure 2c). The building blocks are linked via PO_4 tetrahedra to form a 3-D framework (figures 3 and 4). One cluster is linked to four vanadate chains. The clusters, perpendicular to the chains, connect to the chains at four orthogonal directions. This organization leads to the formation of channels in three directions (figures 3–5, figures S1–S3). Diprotonated piperazine cations and water molecules are in the channels (figure 5, figures S1–S3). The diprotonated piperazine cations interact with the O atoms in the network through H-bonds with the $N \cdots O$ separations from 2.780–3.288 Å. The waters interact with the O atoms in the inorganic network through H-bonds with $O \cdots O$ separation from 2.653–3.096 Å. Extensive hydrogen-bonding interactions between guest molecules and the framework play an important role in forming and stabilizing the 3-D structure. Typical hydrogen bonds are shown in table S1.

3.2. *XPS spectrum analysis*

As shown in the XPS spectra, this sample consists of vanadium and manganese (figures S4–S6). The average oxidation state of vanadium, V_{ox}, can be calculated from the

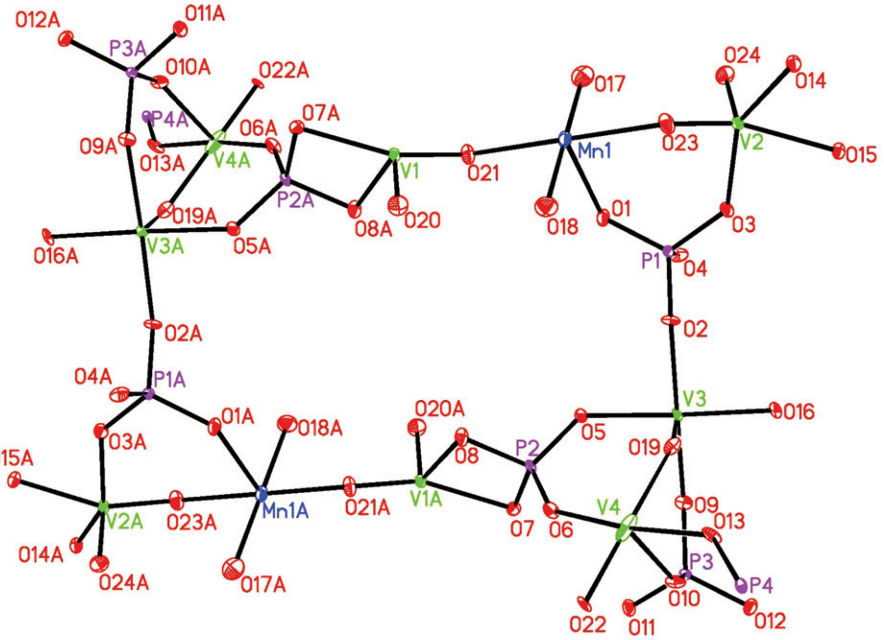

Figure 1. View of a fragment of the molecular structure of **1** showing the geometries of atoms and atomic-labeling scheme. Thermal ellipsoids are shown with 30% probability. C, H, and N are omitted for clarity.

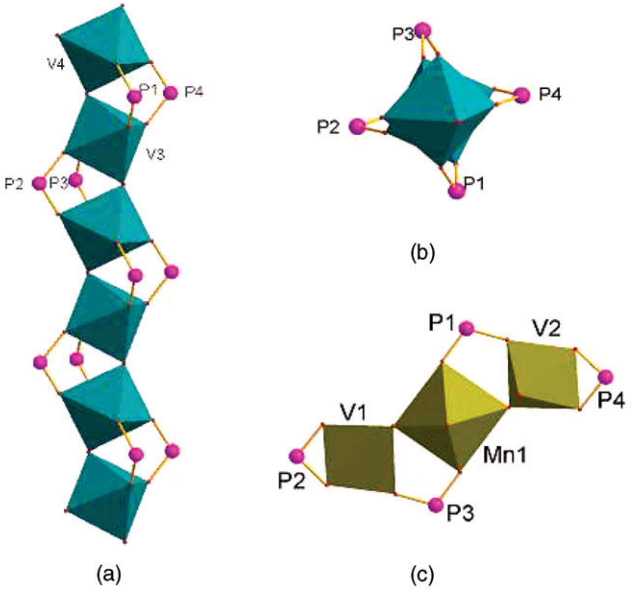

Figure 2. View of two types of building blocks. (a) V^{IV} chains along the *b*-axis constructed from V^{IV} octahedra; (b) vanadate chains along the *a*-axis; and (c) V^{V}–Mn^{II}–V^{V} cluster.

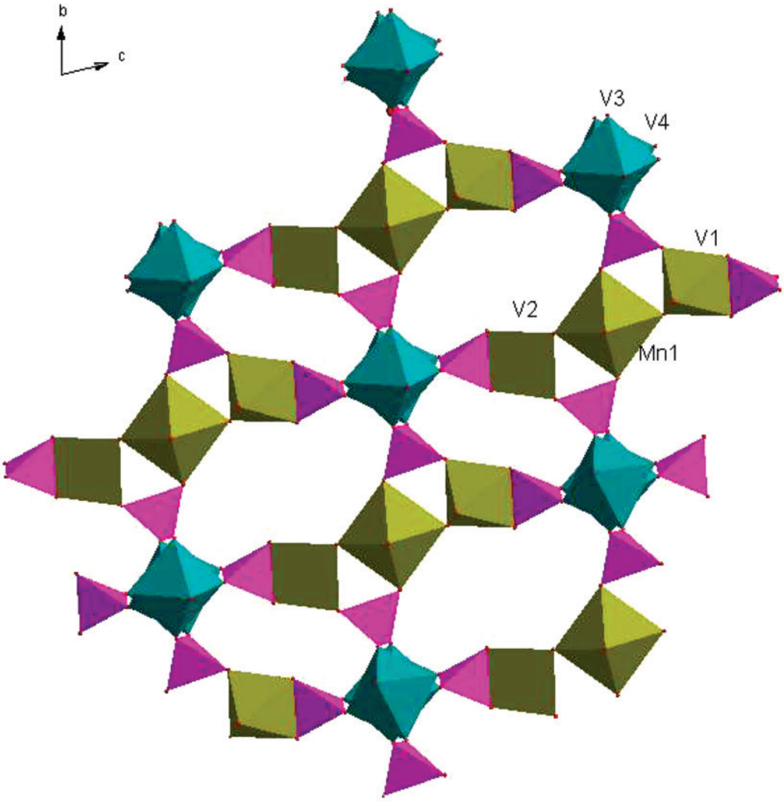

Figure 3. View of the polyhedral diagram down the *a*-axis showing the connection of two types of building blocks.

energy difference between the O1s and V2p3/2 transition centroids, according to the equation [12, 13]:

$$V_{ox} = 13.82 - 0.68[O1s - V2p3/2]$$

The peaks of the binding energy at 522.68 and 536.44 correspond to V2p3/2 and O1s, respectively (table S2). Thus, the average oxidation state of vanadium of the complex is 4.5, which means that V(V) and V(IV) both exist in the structure. The peak at 647.18 eV in the energy region of Mn2p3, as shown in figure S5, is attributed to Mn^{2+}. These conclusions are in good accordance with the valence sum calculation for vanadium and manganese of **1**. Bond valence sum calculations showed that the square pyramidal vanadium has an oxidation state of +5 and the octahedral vanadium has an oxidation state of +4, while the octahedral manganese is indicative of an oxidation state of +2 [14, 15].

3.3. *FT-IR spectroscopy*

As shown in figure S7, the infrared spectrum exhibits characteristic bands from 1312–1639 cm^{-1} associated with the ring stretches of the diprotonated piperazine.

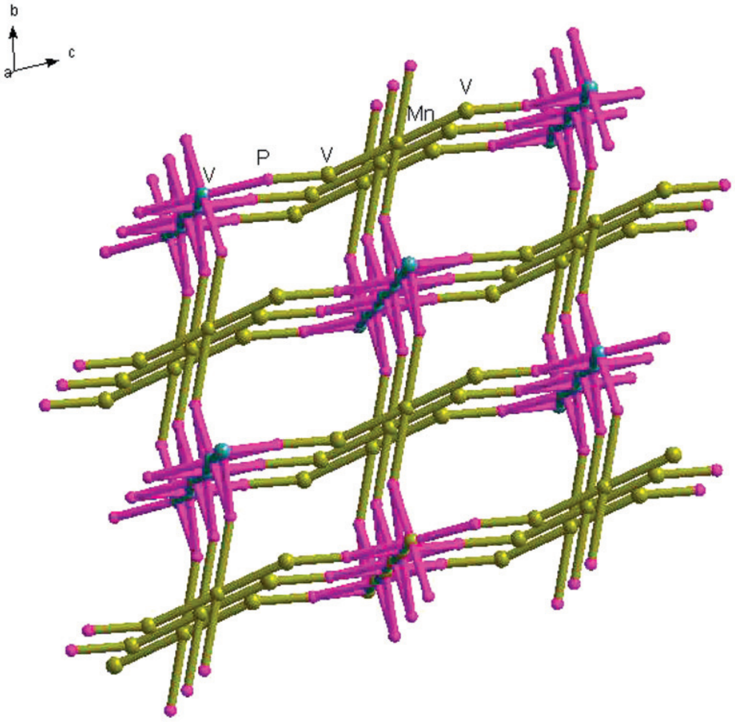

Figure 4. View of 3-D framework of **1**, only showing Mn, V, and P for clarity.

Bands at *ca* 1074 cm^{-1} are attributed to ν(P–O). The bands at 989, 954, and 877 cm^{-1} are attributed to ν(V=O). Multiple bands at 633, 557, 440, 401, and 469 cm^{-1} correspond to asymmetric and symmetric stretching vibrations of bridging metal oxide groups. The positions of the bands and their assignments are consistent with literature reports [16, 17].

3.4. *Thermogravimetric analysis*

Thermogravimetric analysis curve of **1** shows two mass loss steps (figure S8). The first is attributed to the removal of lattice water and ligand water from 260 to 340°C with weight loss of 7.53% (Calcd 7.33%). The next step corresponds to decomposition of diprotonated piperazine, 340–710°C, with weight loss of 17.42% (Calcd 17.53%). The total weight loss (24.95%) is in agreement with the calculated value (24.86%).

3.5. *Fluorescence*

The fluorescence spectrum of solid **1** at room temperature shows that maximum emission occurs at *ca* 393 nm upon excitation at *ca* 243 nm (figure S9). The emission spectrum of **1** may be attributed to an intra-ligand emission instead of ligand-to-metal charge transfer (LMCT) or metal-to-ligand charge transfer (MLCT) since free piperazine exhibits a similar fluorescent emission at 418 nm ($\nu_{ex} = 312$ nm) [18–20].

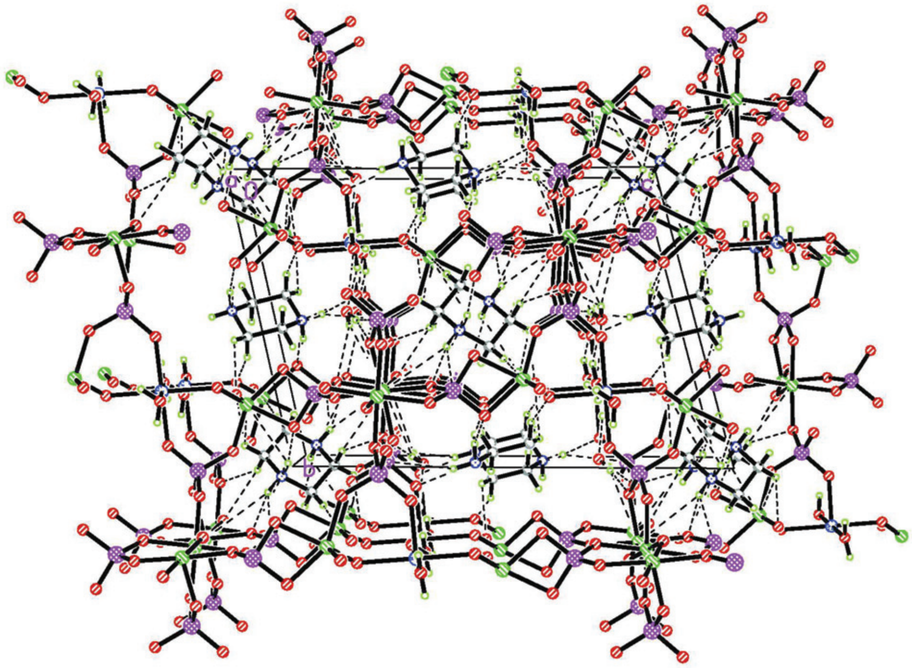

Figure 5. View of the packing diagram down the *a*-axis showing the hydrogen bonding of the diprotonated piperazines and water molecules.

4. Conclusions

A 3-D open framework vanadium-manganese phosphate with the formula $[C_4H_{12}N_2]_2Mn^{II}(V^{V}O_2)_2(V_2^{IV}O_2)(PO_4)_4(H_2O)_4]$ was synthesized under mild hydrothermal conditions. The 1-D chains of V(IV)O_6 octahedra and V^V–Mn^{II}–V^V clusters are linked *via* PO_4 tetrahedra to form channels in three directions. The presence of mixed-valence V(IV)/V(V) sites and 1-D channels in **1** may indicate potential redox catalysis and zeolite-like behavior.

Supplementary material

Crystallographic data for **1** have been deposited with the Cambridge Crystallographic Data Center as supplementary publications, CCDC reference numbers 631359. These data can be obtained free of charge at www.ccdc.cam.ac.uk/conts/retrieving.html (or from the Cambridge Crystallographic Data Centre, 12 Union Road, Cambridge CB2 1EZ, UK; Fax: +44 1223/336 033; E-mail: deposit@ccdc.cam.ac.uk).

Acknowledgments

This work was supported by Scientific Research common program of Beijing Municipal Commission of Education (KM200510028005).

References

[1] S.H. Shi, L. Wang, H.M. Yuan, G.H. Li, J.N. Xu, G.S. Zhu, T.Y. Song, S.L. Qiu. *J. Solid State Chem.*, **177**, 4183 (2004).
[2] R. Finn, J. Zubieta. *Chem. Commun.*, **14**, 1321 (2000).
[3] Y.M. Tsai, S.L. Wang, C.H. Huang, K.H. Lii. *Inorg. Chem.*, **38**, 4183 (1999).
[4] X.M. Zhang, M.L. Tong, S. Feng, X.M. Chen. *J. Chem. Soc., Dalton Trans.*, 2069 (2001).
[5] J.H. Do, R.P. Bontchev, A.J. Jacobson. *J. Solid State Chem.*, **154**, 514 (2000).
[6] Y.J. Cui, Y. Xing, G.H. Li, Y.L. Liu, H. Meng, L. Liu, W.Q. Pang. *J. Solid State Chem.*, **177**, 3080 (2004).
[7] C.H. Huang, L.H. Huang, K.H. Lii. *Inorg. Chem.*, **40**, 2625 (2001).
[8] X.M. Zhang, J.J. Hou, W.X. Zhang, X.M. Chen. *Inorg. Chem.*, **45**, 8120 (2006).
[9] V. Soghomonian, R.C. Haushalter, J. Zubieta, C.J. O'Connor. *Inorg. Chem.*, **35**, 2826 (1996).
[10] G.M. Sheldrick. *SHELXS 97, Program for Crystal Structure Solution*, University of Göttingen, Göttingen (1997).
[11] G.M. Sheldrick. *SHELXL 97, Program for Crystal Structure Refinement*, University of Göttingen, Göttingen (1997).
[12] M.P. Casaletto, S. Kaciulis, L. Lisi, G. Mattogno, A. Mezzi, P. Patrono, G. Ruoppolo. *Appl. Catal., A*, **218**, 129 (2001).
[13] G.W. Coulston, E.A. Thompson, N. Herron. *J. Catal.*, **163**, 122 (1996).
[14] I.D. Brown, D. Altermatt. *Acta Crystallogr., Sect. B*, **41**, 244 (1985).
[15] N.E. Brese, M.O. Shannon. *Acta Crystallogr., Sect. A*, **29**, 266 (1973).
[16] V. Zima, K.H. Lii. *Solid State Chem.*, **172**, 424 (2003).
[17] Y.J. Cui, J. Sun, H. Meng, G.H. Li, C. Chen, L. Liu, X.J. Yuan, W.Q. Pang. *Inorg. Chem. Commun.*, **8**, 759 (2005).
[18] H.Y. Bie, J. Lu, J.H. Yu, J.Q. Xu, K. Zhao, X. Zhang. *J. Solid State Chem.*, **178**, 1445 (2005).
[19] X.M. Ouyang, D.J. Liu, T. Okamura, H.W. Bu, W.Y. Sun, W.X. Tang, N. Ueyama. *J. Chem. Soc., Dalton Trans.*, 1836 (2003).
[20] J.H. Yu, J. Lu, X. Zhang, L. Ye, Q. Hou, J.Q. Xu. *Inorg. Chem. Commun.*, **9**, 415 (2006).